A putative glutathione-binding site in CdZn-metallothionein identified by equilibrium binding and molecular-modelling studies

Marius BROUWER,* Thea HOEXUM-BROUWER and Robert E. CASHON
Duke University School of the Environment, Marine Laboratory/Marine Biomedical Center, Beaufort, NC 28516, U.S.A.

Glutathione (GSH) has been found to form a complex with both vertebrate and invertebrate copper-metallothionein (CuMT) [Freedman, Ciriolo and Peisach (1989) J. Biol. Chem. **264**, 5598–5605; Brouwer and Brouwer-Hoexum (1991) Arch. Biochem. Biophys. **290**, 207–213]. In this paper we report on the interaction of GSH with CdZnMT-I and CdZnMT-II from rabbit liver and with CdMT-I from Blue crab hepatopancreas. Ultrafiltration experiments showed that all three MTs combined with GSH. The measured binding data for the three MTs could be described by a single binding isotherm. The GSH/MT stoichiometry was 1.4 ± 0.3 and $K_{diss.} = 14 \pm 6$ μM. Partially Zn-depleted MT does not significantly bind GSH, indicating that the GSH-binding site is located on MT's Zn-containing N-terminal domain. The putative GSH-binding site on rabbit liver MT was investigated using molecular-graphics analysis. A cleft on the MT's N-terminal domain, which has the labile Zn-2 at its base, could easily accommodate GSH. Cysteine-ligand exchange between the terminal (non-bridging) Cys-26, bound to Zn-2, and the cysteine in GSH is stereochemically possible. Based on these considerations a model of MT–GSH was built in which GSH's cysteine replaces Cys-26 as a terminal Zn-2 ligand. This complex was energy-minimized by molecular-mechanics calculations, taking into account computed partial electrostatic charges on all atoms, including Cd and Zn. These calculations showed that the MT–GSH complex was thermodynamically more stable than MT, due to favourable non-bonded, electrostatic and van der Waals interactions. Six hydrogen bonds can form between GSH and MT. The average pairwise root-mean-square deviations (RMSD) of the metals in energy-minimized MT and MT–GSH, compared with the metals in the crystal structure, were 0.0087 ± 0.0028 nm (0.087 ± 0.028 Å) and 0.0168 ± 0.0087 nm (0.168 ± 0.087 Å) respectively. The RMSD values for the polypeptide-backbone α carbons were 0.0136 ± 0.0060 nm (0.136 ± 0.060 Å) and 0.0491 ± 0.0380 nm (0.491 ± 0.380 Å) respectively. No other docking sites for GSH were found. The energy-minimized structure of an MT–2-mercaptoethanol complex was somewhat less stable than the native MT domain, attesting to the specificity of the MT–GSH interaction. The possible physiological significance of the MT–GSH interaction is discussed.

INTRODUCTION

Metallothioneins (MTs) constitute a family of low-molecular-mass cysteine-rich, metal-binding proteins. MTs are expressed in many different cell lines and tissues following exposure to heavy metals, glucocorticoid hormones, interferon, interleukin-1, bacterial endotoxin, haem–haemopexin and u.v. radiation. MTs appear to be involved in metal detoxification, regulation of Zn and Cu, and donation of metals to apometalloproteins, and possibly in the scavenging of free radicals (Cousins, 1985; Hamer, 1986; Engel and Brouwer, 1989; Waalkes and Goering, 1990; Alam and Smith, 1992). The expression of MT genes is regulated at the transcriptional level, through interactions between cis-acting metal-, glucocorticoid- and haem-responsive elements, and trans-acting DNA-binding, metal-regulatory (metallo)-proteins (Andersen et al., 1990; Seguin, 1991; Butler and Thiele, 1991; Alam and Smith, 1992; Thiele, 1992). N.m.r. spectroscopy (Otvos and Armitage, 1980; Messerle et al., 1990) and X-ray diffraction studies (Robbins et al., 1991) have shown that the Cd/Zn form of mammalian MT is a dumbbell-shaped molecule, composed of an N-terminal, nine-cysteine/three-metal cluster, and a C-terminal, 11-cysteine/four-metal cluster. Each metal is tetrahedrally co-ordinated by four sulphur atoms. There are no contacts between the two metal-binding domains. The CdMT of marine crustacea is composed of two nine-cysteine/three-metal clusters (Otvos et al., 1982). The Cd–thiolate clusters, especially the three-metal cluster in mammalian MT, possess a high degree of dynamic freedom. The continual breaking and re-forming of co-ordination bonds allow for intramolecular metal exchange, primarily within the N-terminal cluster, and intermolecular metal exchange between clusters of different MT molecules (Vasak, 1986; Otvos et al., 1989). Differences in exchange rates strongly suggest that the two domains of mammalian MTs have evolved to perform different functional roles. The kinetically labile N-terminal domain may function in metal-exchange processes, whereas the kinetically stable C-terminal domain is important in detoxification. Studies on mutant MTs in which cysteine residues in either domain have been replaced corroborate this conclusion (Cismowski and Huang, 1991; Cismowski et al., 1991). Whether intracellular metal exchange occurs between MTs or between MT and (apo)metalloproteins is unknown.

Recent studies have demonstrated the existence of intracellular Cu(I)MT–GSH and Cu(I)–GSH complexes in mammalian cell lines (Freedman et al., 1989) and in the hepatopancreas (digestive gland) of marine crustacea (Brouwer and Brouwer-Hoexum, 1991, 1992). Cu(I)–GSH is proposed as an intracellular source of Cu for the biosynthesis of Cu-dependent proteins, and Cu(I)–GSH may be derived from the Cu(I)–MT pool under Cu-deficient conditions. We have found that GSH forms a stable ($K_{diss.}$ value of 1 μM) 1:1 complex with CuMT-III from the American lobster, *Homarus americanus*. CuMT isoforms I and II form a transient MT–GSH complex which may

Abbreviations used: MT, metallothionein; MSH, 2-mercaptoethanol; DTT, dithiothreitol; DTNB, 5,5′-dithio-bis(2-nitrobenzoic acid); RMSD, root-mean-square deviation.

* To whom correspondence should be addressed.

release copper as a Cu(I)–GSH complex. The latter can restore the oxygen-binding capacity of Cu-free haemocyanin, whereas CuMT cannot (Brouwer and Brouwer-Hoexum, 1991, 1992).

Mammalian CuMT contains 12 Cu atoms (Nielson et al., 1985; Kille et al., 1992), which are trigonally co-ordinated to cysteine residues of MT (Abrahams et al., 1986). Lobster CuMT binds 10 Cu atoms (Brouwer and Brouwer-Hoexum, 1991). These observations raise the question whether the interaction between GSH and MT is specific for the Cu-containing MTs, or whether this is a general phenomenon that also occurs with the Cd/Zn-containing MTs. In view of this we have examined/characterized the structural and physical chemical properties of the interaction between GSH and CdMT from the Blue crab, *Callinectes sapidus*, and CdZnMT from the rabbit, *Oryctolagus cuniculus*. Both the invertebrate and mammalian CdMTs were found to complex with GSH. A putative GSH-binding site on the N-terminal domain of MT has been identified by molecular-graphics analysis.

EXPERIMENTAL

Preparation of CdZnMT

Cd_6MT-I was isolated from the hepatopancreas of Blue crabs (Brouwer et al., 1992). CdZnMT-I/II isolated from rabbit liver was a gift from Dr. F. A. Liberatore, E. I. Dupont, Medical Products Department, Billerica, MA, U.S.A. The protein had been purified by ethanol precipitation, gel-permeation chromatography and batch-wise elution from a DEAE-cellulose column. The protein was thus a mixture of CdZnMT-I and CdZnMT-II. The two isoforms were separated by anion-exchange chromatography as described before (Brouwer et al., 1992).

Repair of partially oxidized MT

CdZnMT from rabbit liver appeared to have lost some of its Zn (see the Results section). To restore its full metal-binding complement, a solution of 10 mg of CdZnMT in 2 ml of N_2-saturated 10 mM Hepes/50 mM NaCl, pH 7.4, was incubated with 5 mM dithiothreitol (DTT) and 1.5 mM $ZnCl_2$ at room temperature for 10 min. The mixture was then chromatographed on a Sephadex G-50 column (1.6 cm × 58 cm) in 10 mM Tris/HCl (pH 7.0) at a flow rate of 15 ml/h. Fractions containing monomeric MT were pooled and separated into CdZnMT-I and CdZnMT-II by anion-exchange chromatography on a DEAE-cellulose column (2.5 cm × 20 cm) using a 1 litre gradient of 10–200 mM Tris/HCl (pH 7) at a flow rate of 35 ml/h. The CdZnMT isoforms were dialysed against 10 mM Hepes/50 mM NaCl (pH 7.4) before GSH-binding experiments were performed. All procedures were carried out in N_2-saturated buffers at 4 °C.

The Cd/Zn ratio in the Zn-reconstituted MT was measured by atomic absorption spectroscopy. The amount of Zn bound to the cysteine residues of MT was determined by u.v. spectroscopy. $CdCl_2$, giving a final concentration of 50 μM Cd, was added to a degassed solution of 10 μM CdZnMT in 10 mM Hepes (pH 7.4), and the u.v. absorbance spectrum from 220 to 300 nm was recorded. The amount of thiolate-bound Zn displaced by Cd was calculated from the increase of the absorbance value at 250 nm using a molar absorptivity for the Cd–$(thiolate)_4$ complex at 250 nm of 14500 (Vasak et al., 1981).

GSH-binding studies

Solutions containing 3–8 μM rabbit liver CdZnMT-I and CdZnMT-II and Blue crab CdMT-I in 10 mM Hepes/50 mM NaCl (pH 7.4) in the presence of different concentrations of GSH were subjected to ultrafiltration, in the cold, in a 10-ml-capacity Amicon cell with a 2.5-cm-diam. YM-10 membrane as described previously (Brouwer and Brouwer-Hoexum, 1991). MT concentrations were calculated assuming seven metal atoms/rabbit MT and six metal atoms/crab MT. Retentate and filtrate were analysed for GSH using the enzymic recycling assay in the presence of 5,5′-dithiobis(2-nitrobenzoic acid) (DTNB) (Anderson, 1985). It was found that the assay of the retentate was inhibited, possibly by the reaction of DTNB with the cysteine residues of MT. To correct for this apparent loss of GSH, GSH was assayed in the retentate after the addition of a known amount of GSH as an internal standard. If we assume that the GSH concentration in the retentate is z μM, and that the efficiency of the assay is a%, then $az = b$, where b is the measured concentration of GSH. After the addition of c μM GSH to the retentate we have $a(z+c) = m$, where m is the GSH concentration measured in the presence of the internal standard. From these two equations it follows that the efficiency is $a = (m-b)/c$. The GSH concentration in the retentate is thus $z = b/a$. GSH was found to be freely permeable through the YM-10 membrane, and no loss of GSH was observed when GSH was subjected to ultrafiltration in the absence of CdMT. The YM-10 membranes were virtually impermeable to CdZnMT. The percentage of total Cd in the filtrates was 4.28 ± 1.13% ($n = 13$). It is possible to correct for the effect of this slight permeability of CdZnMT on the calculated amounts of free and bound GSH (Brouwer and Brouwer-Hoexum, 1991). However, the correction did not significantly alter the outcome of the data analysis, and was therefore not necessary.

In principle, to determine the amount of GSH bound to MT, it is not necessary to measure the GSH concentration in the retentate. We know the amount of GSH, and MT, present in the equilibrium mixture before the ultrafiltration step: GSH_{added} and MT_{added}. During ultrafiltration, the ratio of GSH–MT to MT does not change since both are concentrated to the same extent during the concentration step. This implies that the free GSH concentration does not change during the ultrafiltration step. Therefore, the GSH concentration in the filtrate is equal to the concentration of free GSH in the mixture before ultrafiltration. From this it follows that $[GSH]_{bound} = [GSH]_{added} - [GSH]_{filtrate}$ and $GSH/MT = [GSH]_{bound}/[MT]_{added}$.

Data were analysed according to $r = nK[GSH]_{free}/(1 + K[GSH]_{free})$, using standard non-linear least-squares minimization, where r is $[GSH]_{bound}/MT$, $[GSH]_{free}$ is the concentration of free GSH, n is the number of GSH-binding sites/MT, and K is the binding constant for the MT–GSH complex.

Molecular-graphics analysis and energy minimization

Graphics modelling was performed interactively on an Evans and Sutherland ESV Workstation, using the Graphics program SYBYL (version 5.5, Tripos Associates, St. Louis, MO, U.S.A.). Energy minimization by molecular-mechanics calculations was performed using SYBYL's MAXIMIN2 function. To evaluate the effect of the electrostatic charges of the metals on the minimized structures, three different energy-minimization calculations were performed. In the first one, electrostatic charges were completely ignored. In the second one, the metals were each assigned a point charge of +2 and the distribution of electrostatic charges on all other atoms was calculated using the method of Gasteiger and Marsili (1980). In the third one, the metals were included in the calculation of the charge distribution. Further details of these procedures are provided in the Discussion section. Minimizations, starting with the crystal structure, were carried out in the TRIPOS force-field, using the conjugate gradient method (Kini and Evans, 1991). The bridging and terminal

sulphur atoms were assigned a tetrahedral environment with one and two lone electron pairs respectively (Arseniev et al., 1988; Messerle et al., 1990). The S–Me^{2+}–S angles (where Me^{2+} is the metal ion) were constrained to the values obtained from the crystal structure (Robbins et al., 1991). The Cd–S and Zn–S equilibrium bond lengths were set to 0.2511 nm (2.511 Å) and 0.2378 nm (2.378 Å), which are the average Cd–S and Zn–S bond lengths in the crystal structure. All of the calculations employed a dielectric constant of 1 for the evaluation of the electrostatic energy. All other parameters for minimization were the default parameters in SYBYL. At present it is quite difficult to make calculations in the presence of explicit solvent molecules. Therefore calculations were carried out on the structure of MT and the MT–GSH complex in the absence of water. The present calculated structure should be viewed with this limitation in mind. Structures were refined until the final energy change was less than 0.0001 kcal/mol. The protein structures obtained after energy minimization were compared with the experimental structure by superposition of the minimized structure on to the crystal structure using a least-squares fit for all α carbons. The root-mean-square deviation (RMSD) is used as an estimate of fit.

RESULTS

Restoration of oxidized CdZnMT

The Cd/Zn ratio of the purified rabbit MT was approx. 6, which is much higher than the 5/2 stoichiometry generally found in CdZnMT in solution (Winge and Miklossy, 1982a) and in the crystal structure (Robbins et al., 1991). This suggested that the labile Zn (Li et al., 1980) had been lost from the protein. To evaluate this possibility, and to restore the metal-binding capacity of MT, 25 μM CdZnMT was reduced with 1 mM 2-mercaptoethanol (MSH) at pH 8 for 3 h at 37 °C and subsequently incubated for 5 h with different concentrations of $ZnCl_2$ at room temperature, followed by size-exclusion h.p.l.c. to separate MT from Zn and MSH. The Cd/Zn ratio decreased from 7 to 4 (at 400 μM Zn). The decrease in the Cd/Zn ratio was found to be associated with an increase in Zn, whereas the amount of Cd bound to the protein remained unchanged. The amount of Zn was measured by atomic absorption spectroscopy and calculated from the change in u.v. absorption that accompanies displacement of Zn by Cd. The measured and calculated values were identical, indicating that all the Zn was bound as zinc tetrathiolate.

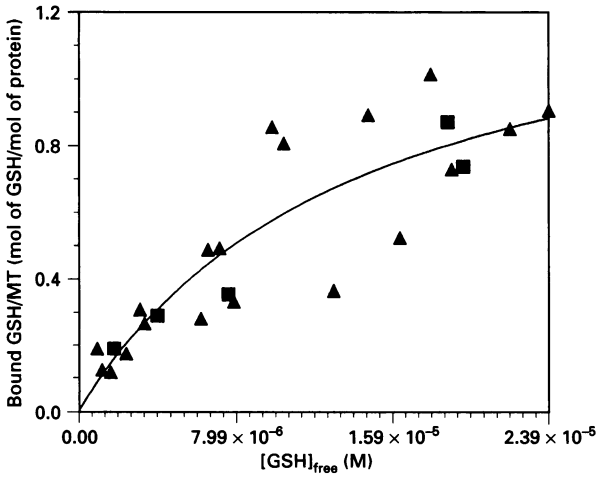

Figure 1 GSH binding to CdZnMT and CdMT

Binding of GSH to rabbit liver CdZnMT (▲) and Blue crab CdMT (■) was evaluated by ultrafiltration experiments. The line was calculated with a $K_{diss.}$ value of 14 μM and a GSH/MT value of 1.4, determined from the data by non-linear least-squares minimization.

When CdZnMT was reduced, followed by size-exclusion h.p.l.c. and subsequent incubation with Zn, no restoration of Zn-binding capacity was observed. These experiments suggest that MSH reduces disulphide bridges in oxidized MT. Once the MSH has been removed the reduced thiol residues (or thiol and mixed disulphide) rapidly re-oxidize. Reduction of protein disulphides is often unfavourable, due to the high value for $k_{intra.}$, i.e. the rate constant for the reaction of the protein thiol group with the protein S–S–M, mixed disulphide group (Creighton, 1986).

The re-oxidation of protein thiol groups can be prevented by carrying out the reduction with DTT, which has two thiol groups on the same molecule. In this case the protein mixed disulphide reacts to give protein–SH and oxidized DTT. Using DTT and the conditions as described in the Experimental section we obtained CdZnMT-I and CdZnMT-II preparations with Cd/Zn ratios of 2.50 and 2.42 respectively. The amount of Cd bound to the MTs remained unchanged. U.v. titration with Cd showed that all of the Zn was bound as zinc tetrathiolate.

GSH-binding experiments

GSH-binding studies, by means of ultrafiltration experiments, were carried out with restored CdZnMT-I and CdZnMT-II from rabbit liver and with CdMT from the Blue crab *Callinectes sapidus*. The assays for GSH in the retentates, which contain MT and GSH, were inhibited, whereas those in the filtrates were not. Such inhibition was not observed during studies of the binding of GSH to CuMT (Brouwer and Brouwer-Hoexum, 1991). The reason for the inhibition is not clear, but is probably, at least in part, due to the reaction of DTNB with the thiol groups of CdZnMT in the presence of EDTA. The latter is a component of the assay mixture and is known to remove metals from CdZnMT (Li et al., 1980; Winge and Miklossy, 1982a). CuMT does not react with DTNB to a noticeable extent under the same conditions. When the amount of GSH bound to MT was calculated with the eqns. $[GSH]_{bound} = [GSH]_{added} - [GSH]_{filtrate}$ and $GSH/MT = [GSH]_{bound}/[MT]_{added}$ (see the Experimental section), numerical analysis of the binding data by non-linear least-squares minimization gave a $K_{diss.}$ value of 14 ± 6 μM, and a GSH/MT ratio of 1.41 ± 0.32 (Figure 1). Analysis of the results with the assumption of two classes of independent binding sites for GSH did not improve the fit between measured and calculated data. When $[GSH]_{bound}$ was measured, using an internal standard to correct for inhibition of the GSH assay, analysis of the data gave the same, but less accurate, results: $K_{diss.} = 32 \pm 26$ μM, and $GSH/MT = 1.52 \pm 0.32$. The GSH-binding data obtained with *C. sapidus* CdMT and rabbit liver CdZnMT-I and CdZnMT-II are described by the same binding isotherm, indicating that the three different MTs interact to the same extent with GSH.

Molecular-graphics analysis

GSH-binding studies with partially oxidized, and partially Zn-depleted CdZnMT, showed that the maximum amount of GSH bound/MT did not exceed 0.2 mol of GSH/mol of MT. Reduction of MT and re-introduction of Zn into the molecule increased the GSH-binding capacity to 1.4 ± 0.3 GSH/MT. This strongly suggests that the labile Zn site needs to be occupied for GSH binding to occur. Zn is bound to MT's N-terminal domain, and interactions between the N- and C-terminal metal-binding domains do not occur (Messerle et al., 1990; Robbins et al.,

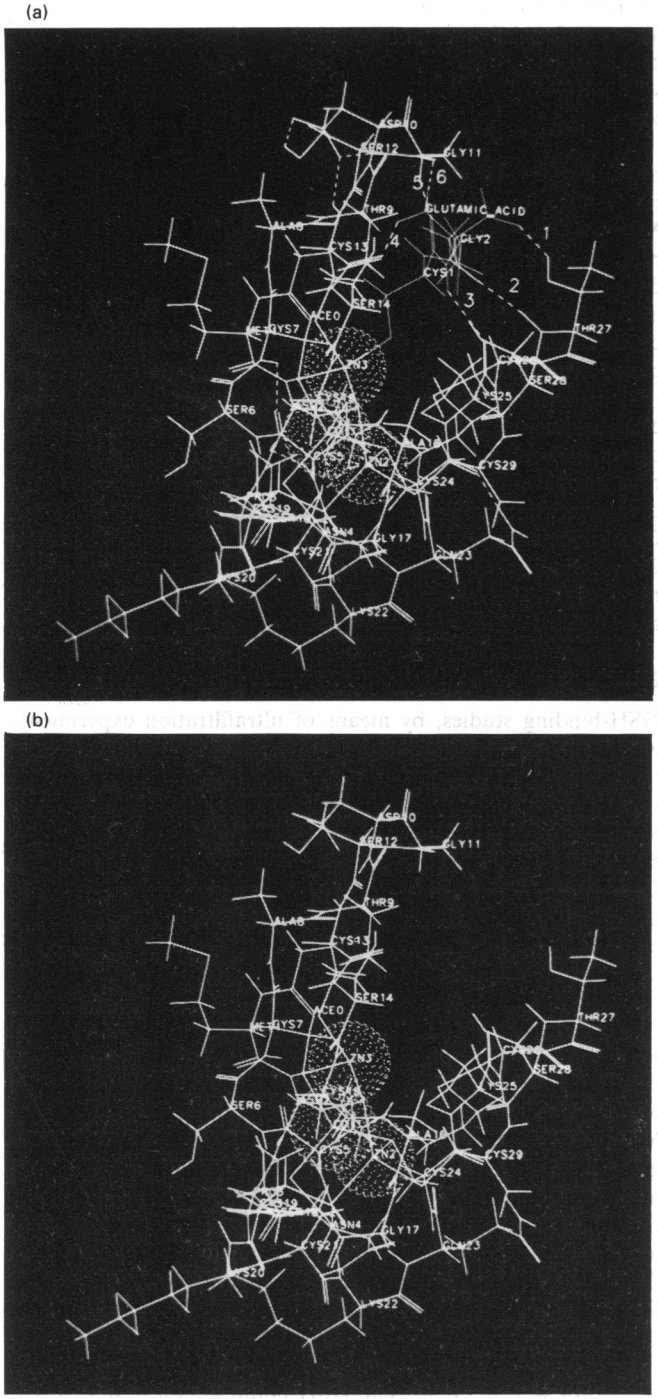

Figure 2 Structure of the GSH–MT complex

(**a**) Calculated structure of the complex between GSH and the N-terminal domain of MT. The residues labelled GLUTAMIC ACID, CYS1 and GLY2 represent the GSH molecule. The three metals are indicated by the dotted spheres. The labels Zn-2 and Zn-3 correspond to Zn-1 and Zn-2 of the crystal structure. GSH is bound to MT by means of a metal thiolate bond between CYS1 and Zn-2. Broken lines numbered 1–6 delineate hydrogen bonds that stabilize the MT–GSH complex. The six hydrogen bonds are listed in Table 1. The potential-energy terms of the energy-minimized complex are listed in Table 2. (**b**) N-terminal domain without GSH. Structures (**a**) and (**b**) are shown to help indicate the location of the GSH-binding cleft.

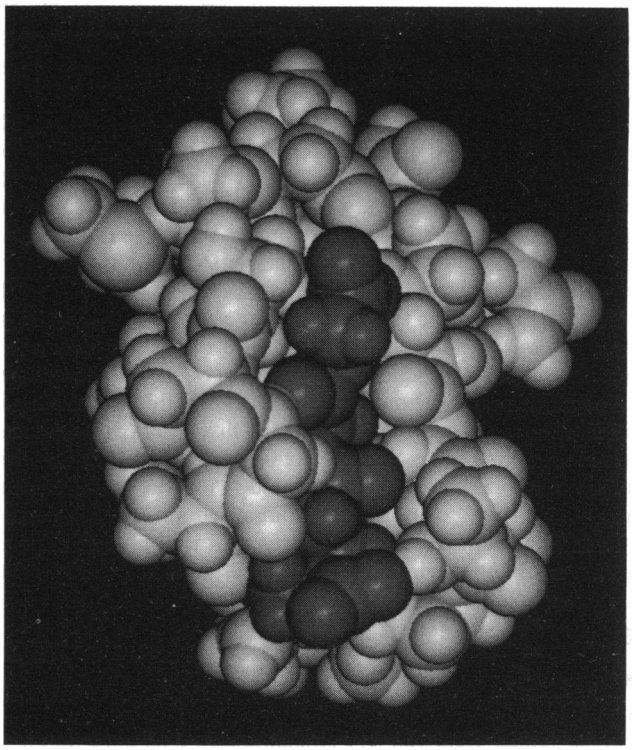

Figure 3 Space-filling model of the energy-minimized MT–GSH complex

Dark spheres represent the GSH molecule. This view is derived from the structure shown in Figure 2(a) by rotation of the structure around the *x*-axis by 90°. The Gly-Cys-Glu residues of GSH run from top to bottom.

Table 1 Hydrogen bonds between GSH and MT

Number of bond refers to the structure shown in Figure 2.

	Amino acid/atom					
Bond	GSH			MT		
1	Glu	C=O	α-Carboxyl	Thr-27	H–O	Hydroxyl
2	Glu	C=O	γ-Carbonyl	Thr-27	H–N	Amide
3	Gly	N–H	Amide	Lys-25	O=C	Carbonyl
4	Glu	N–H	α-Amino	Cys-13	O=C	Carbonyl
5	Cys	C=O	Carbonyl	Gly-11	H–N	Amide
6	Glu	N–H	α-Amino	Gly-11	O=C	Carbonyl

1991). Molecular-modelling studies were therefore carried out with the N-terminal domain (residues 1–29). Inspection of this domain revealed a cleft that could easily accommodate GSH. The labile Zn atom, ligated by Cys-7, -13, -15 and -26, is found at the base of the cleft. Metal–thiolate clusters in MT and inorganic cage complexes have a considerable degree of dynamic freedom, characterized by temporary breaking and forming of co-ordination bonds (Hagen et al., 1982; Vasak, 1986; Otvos et al., 1989). To build a molecular model of the MT–GSH complex we removed the bond between Zn-2 and Cys-26 and attached the cysteine sulphur of GSH to the open co-ordination site on the Zn atom. This complex was subjected to molecular-mechanics calculations. The S–metal–S angles were maintained at the values obtained from the crystal structure. The S(MT)–Zn–S(GSH) angles were kept at the same values as those for the S–Zn–S(Cys-26) angles. Partial charges on all atoms, including the three metals, were calculated as described in the Discussion section.

Table 2 Potential energy terms of energy-minimized MT and MT–GSH complex (kcal/mol)

Both structures were minimized in the TRIPOS force-field. Charges on all atoms, including metals, were calculated as described in the text. 1 kcal/mol = 4.2 kJ/mol.

	Potential energy (kcal/mol)	
Energy term	MT*	MT–GSH†
Bond-stretching energy	9.704	10.356
Angle-bending energy	54.558	68.595
Torsional energy	72.115	71.523
Out-of-plane-bending energy	1.322	1.736
1–4 van der Waals energy	25.689	28.425
van der Waals energy	−90.848	−105.508
1–4 Electrostatic energy	136.723	134.660
Electrostatic energy	−298.994	−418.916
Fixed-angle energy	0.005	0.003
Total potential energy	−89.726	−209.122

* N-terminal domain (residues 1–29).

† The bond between Cys-26 and Zn-2 was clipped. The cysteine sulphur of GSH was attached to the open co-ordination site on the Zn.

The structure of the energy-minimized complex is shown in Figures 2 and 3. The complex is stabilized by six hydrogen bonds between GSH and MT (Figure 2 and Table 1). The calculated potential energy terms of the two energy-minimized structures are listed in Table 2. The MT–GSH complex is energetically favoured over the free domain due to non-bonded van der Waals and electrostatic interactions.

DISCUSSION

GSH has been implicated in protection against Cd- and Cu-induced toxicity (Singhal et al., 1987; Freedman et al., 1989) and in tumour-cell resistance to metal-based anti-cancer drugs (Godwin et al., 1992). The existence of intracellular Cu(I)–GSH and CuMT–GSH has been reported for both mammals and invertebrates (Freedman et al., 1989; Brouwer and Brouwer-Hoexum, 1991, 1992). The Cu(I)–GSH complex may act as a source of Cu for the biosynthesis of CuMT (Freedman et al., 1989), haemocyanin (Brouwer and Brouwer-Hoexum, 1991, 1992) and superoxide dismutase (Steinkuhler et al., 1991). Whether or not GSH binds to CdZnMT was unknown. The data reported in this study demonstrate that GSH can bind to both invertebrate (Blue crab) and vertebrate (rabbit) CdZnMT. A full complement of metals bound to the N-terminal domain of MT was prerequisite for binding to occur. The stoichiometry and binding constant for the CdZnMT–GSH interaction (GSH/MT = 1.4 ± 0.3 and $K_{diss.} = 14 \pm 6$ μM) showed rather large S.D. values. This may, at least in part, be due to the difficulty of assaying GSH in the presence of CdZnMT and to the non-rigid, dynamic organization of the metal–thiolate clusters in the N-terminal domain of MT. Several interchangeable structural MT isoforms may co-exist (Vasak, 1986), which may interact to a different extent with GSH. The results obtained from our ultrafiltration experiments have been confirmed by size-exclusion h.p.l.c. of GSH, and mixtures of GSH and CdZnMT-I or CdZnMT-II. The amount of free GSH, which can be determined reliably, decreases considerably when GSH and MT are co-chromatographed. No measurable release of Cd or Zn was observed during our experiments.

Part of the Zn in the N-terminal domain of CdZnMT is extremely reactive with EDTA (Li et al., 1980; Winge and Miklossy, 1982a,b). The solvent accessibilities of the sulphur atoms bonded to Zn-1 and Zn-2, which may be a useful indicator of preferred sites of metal-exchange reactions, are 0.00505 nm^2 (5.05 Å^2) for Zn-1 and 0.3583 nm^2 (35.83 Å^2) for Zn-2 (Robbins et al., 1991). This strongly suggests that Zn-2 represents the reactive Zn atom. The fact that partially Zn-depleted MT does not combine to a significant degree with GSH led us to postulate that Zn-2 is part of the GSH-binding site. Molecular-graphics analysis revealed that this Zn atom was at the bottom of a cleft that could easily accommodate GSH. It was found to be impossible to dock GSH at either Zn-1 or Cd. Based on the known dynamic nature of the metal–thiolate cluster in the N-terminal domain of MT, which involves breaking and reforming of metal-to-cysteine bonds, we hypothesized that the cysteine sulphur of GSH might compete with one of the terminal cysteine (Cys-13 or Cys-26) sulphurs for a co-ordination site on Zn-2. We found that such cysteine-ligand exchange was stereochemically possible between GSH and Cys-26, but not between GSH and Cys-13. Based on these considerations the Zn-2–Cys-26 bond in MT was broken and replaced with a Zn-2–Cys(GSH) thiolate bond. This complex was then energy-minimized by molecular-mechanics calculations using the TRIPOS force-field.

The TRIPOS valence force-field expresses the total potential energy of a molecule as the sum of the bond-stretching, angle-bending, out-of-plane-bending, torsional and non-bonded (van der Waals, and electrostatic) terms. The application of empirical force-field computations to metal co-ordination compounds is problematic because of the large variation of ligand–metal–ligand bond angles observed at transition-metal centres (Lauher, 1986; Allured et al., 1991). Energy minimization of the CdZnMT was therefore carried out keeping the sulphur–metal–sulphur angles constrained to the values found in the crystal structure. The fixed-angle constraint introduced in this way was almost negligible (Table 1).

It is unsuitable in molecular-dynamics and -mechanics calculations of simple metal complexes and metalloproteins to assign the formal charges +2 to Cd and Zn. Quantum-mechanical calculations on a series of metal complexes, including zinc thiolate compounds, indicate that the computed charges on the metals are generally much less than the formal charges (Fischer-Hjalmars and Henriksson-Enflo, 1982). Partial charges for the active site of metalloproteins are generally obtained from calculations *ab initio* for a simplified but representative model that mimics the metal-ligand structure of the protein. These charges can then be used in molecular-mechanics and -dynamics calculations (Shen et al., 1990; Hoops et al., 1991; Banci et al., 1992).

To evaluate the importance of charge in the energy minimization of MT, the structure of MT was calculated in three different ways. In the first procedure electrostatic charges were ignored. In the second procedure the three metals were assigned a formal point charge of +2, and were not included in the computation of the charge distribution. The atomic charges of all other atoms were calculated according to the method of partial equalization of orbital electronegativity (Gasteiger and Marsili, 1980), as implemented by SYBYL. In the third procedure the metals were included in the calculation of the charge distribution, which requires knowledge of the electronegativities of the neutral, anionic and cationic forms of Cd and Zn in their tetrahedral valence state. Since these values are not known, we chose to use the corresponding values for the ground state as a first, empirical, approximation. The electronegativity values for the uncharged atoms were obtained from Lange's Handbook of Chemistry (1973). Electronegativities of the cation and anion were calculated using Mulliken's definition: $X = 1/2(I+E)$, where I and E are the ionization potential and electron affinity respectively. The

Table 3 RMSD values between α-carbon atoms and metal atoms of the crystal structure and energy-minimized structures

All values are expressed in Angstroms (1 Å = 0.1 nm).

Residue/metal	MT*	MT†	MT‡	MT–GSH§
Met-1	0.168	0.290	0.259	0.617
Asp-2	0.064	0.201	0.263	0.358
Pro-3	0.105	0.386	0.167	0.539
Asn-4	0.091	0.249	0.131	0.214
Cys-5	0.120	0.159	0.065	0.185
Ser-6	0.051	0.548	0.102	0.385
Cys-7	0.086	0.345	0.083	0.192
Ala-8	0.043	0.209	0.051	0.290
Thr-9	0.088	0.167	0.095	0.113
Asp-10	0.128	0.161	0.116	0.388
Gly-11	0.114	0.069	0.052	0.645
Ser-12	0.069	0.121	0.083	0.739
Cys-13	0.179	0.413	0.173	0.606
Ser-14	0.102	0.110	0.097	0.538
Cys-15	0.108	0.050	0.133	0.390
Ala-16	0.054	0.092	0.158	0.547
Gly-17	0.103	0.149	0.161	0.319
Ser-18	0.073	0.285	0.099	0.413
Cys-19	0.197	0.506	0.209	0.336
Lys-20	0.111	0.189	0.180	0.555
Cys-21	0.169	0.226	0.156	0.300
Lys-22	0.159	0.189	0.238	0.344
Gln-23	0.144	0.194	0.161	0.277
Cys-24	0.182	0.209	0.081	0.155
Lys-25	0.069	0.206	0.063	0.464
Cys-26	0.144	0.144	0.185	1.424
Thr-27	0.070	0.105	0.073	1.148
Ser-28	0.139	0.307	0.106	1.393
Cys-29	0.150	0.474	0.146	0.393
Average RMSD	0.113	0.236	0.136	0.492
Cd	0.145	0.318	0.117	0.129
Zn-1	0.101	0.211	0.061	0.107
Zn-2	0.076	0.306	0.083	0.267
Average RMSD	0.107	0.278	0.087	0.168

* Atomic electrostatic charges were not included in the energy-minimization calculations.

† Zn and Cd were assigned point charges of +2. Charges on other atoms were calculated according to Gasteiger and Marsili (1980).

‡,§ Metals were included in the calculation of charge distribution (see text for details).

ionization potentials (*I*) for the neutral and cation forms were obtained from the CRC Handbook of Chemistry and Physics (1984). The electron affinity of the neutral atom was assumed to be equal to −1.54 eV, the value reported for Hg, another $d^{10}s^2$ atom (Lange, 1973). In this way the electronegativities for Me^-, Me, and Me^+ (where Me is a metal atom), were −0.75, 2.856 and 12.951 eV for Cd and −0.75, 2.560 and 13.679 eV for Zn. When these values were used to calculate charge distributions on all the atoms in MT, the formal charge on Zn and Cd decreased from +2 to 0.302 and 0.425 respectively, which is very close to the value calculated *ab initio* for a $[Zn(S)_4]^{2-}$ complex (see Figure 8 in Fischer-Hjalmars and Henriksson-Enflo, 1982). The net charge on the Me_3S_9 cluster, taking into account the charge on the cysteine C^β atoms, was −2.81, which is close to the expected charge of a complex formed from three bivalent metal ions and nine thiolate ligands.

The average pairwise RMSD value calculated for the three metals in the crystal structure and energy-minimized, uncharged structure was 0.0107±0.0035 nm (0.107±0.035 Å) (Table 3). If computed atomic charges were included in the energy minimization, this value reduced to 0.0087±0.0028 nm (0.087±0.028 Å). For the point-charge, Cd^{2+}/Zn^{2+} model, the RMSD for the three metals increased to 0.0278±0.0059 nm (0.278±0.059 Å). The average RMSD value for the α carbons in the crystal and energy-minimized structure was 0.0136 nm (0.136 Å). The average RMSD value for the metals in the energy-minimized MT–GSH complex, compared with the crystal structure, was 0.0168±0.0087 nm (0.168±0.087 Å), with the largest deviation observed for the Zn-2 atom. The average RMSD for the α carbons was 0.0492±0.0328 nm (0.492±0.328 Å), with the largest deviations observed for Cys-26, Thr-27 and Ser-28 (Table 3). The MT–GSH complex was stabilized by six hydrogen bonds between GSH and MT (Table 1). Thermodynamically the MT–GSH complex was more stable than MT mainly due to favourable electrostatic interactions, and to a lesser extent, to van der Waals interactions (Table 2). Since GSH binds more tightly to anion-exchange columns than MT (Freedman et al., 1989), ion-exchange chromatography may result in disruption of the electrostatically stabilized CdZnMT–GSH complexes. It should be noted that the electrostatic energy term was calculated with a value of 1 for the dielectric constant. This may explain, at least in part, the large discrepancy between the free energy of GSH binding ($\Delta G = -6.6$ kcal/mol) and the calculated energy difference between the two structures (−119 kcal/mol). Energy-minimization calculations on an MT–MSH complex showed the complex to be slightly less stable than MT itself, further attesting to the specificity of the MT–GSH interaction.

The most important question that remains to be answered concerns the physiological significance of the interaction between MT and GSH. Cu(I)–GSH may deliver Cu(I) for formation of Cu(I)–MT, for the biosynthesis of other Cu-dependent proteins (Freedman et al., 1989; Steinkuhler et al., 1991), and under Cu-deficient conditions the Cu(I)–GSH complex may be derived from the intracellular Cu(I)–MT pool (Brouwer and Brouwer-Hoexum, 1991, 1992). It is tempting to speculate that a similar situation exists for the participation of ZnMT and GSH in the biosynthesis of Zn proteins. However, we know little about the equilibria that exist between intracellular free Zn, ligand–Zn complexes, ZnMT and the proteins in which Zn has a functional role (Coleman, 1992). Similarly we do not know whether Zn gradients exist between cell compartments or cells. Studies *in vitro* have shown that ZnMT is reactive in ligand-substitution reactions with apo-Zn-proteins as competing ligands (Li et al., 1980; Winge and Miklossy, 1982a). Evidence that such chemistry may also occur in cells has been reported (Krezoski et al., 1988; Kraker et al., 1988). The latter studies show that ZnMT is a labile depot of Zn in the Ehrlich cell which can be mobilized under Zn-deficient conditions. Whether GSH plays a role in the mobilization process is not known. Our measurements, which show that GSH does not remove Zn or Cd from MT under the experimental conditions used in this study, seem to argue against this possibility. However, GSH can remove Zn from CdZnMT after multiple ultrafiltration steps, which forces the equilibrium between GSH and CdZnMT towards the formation of a Zn–GSH complex (Brouwer et al., 1993). In addition to directly participating in the intracellular distribution of Zn, GSH may act as an allosteric effector which serves to lower the metal-binding affinity of MT, or to increase the rate of turnover of MT by making the protein more susceptible to proteolytic digestion, thereby indirectly promoting the release of metals. Current work in our laboratory is directed at further clarifying the physiological significance of the interaction between MT and GSH.

This work was supported by NIH grants ES 04074 (M.B.) and ES 01908 (Marine Biomedical Center). The molecular-graphics facility of the Marine Biomedical Center is supported by a grant from the McGregor Foundation.

REFERENCES

Abrahams, L., Bremner, I., Diakun, G. P., Garner, C. D., Hasnain, S. S., Ross, I. and Vasak, M. (1986) Biochem. J. **236**, 585–589

Alam, J. and Smith, A. (1992) J. Biol. Chem. **267**, 16379–16384

Allured, V. S., Kelly, C. M. and Landis, C. R. (1991) J. Am. Chem. Soc. **113**, 1–12

Andersen, R. D., Taplitz, S. J., Oberbauer, A. M., Calame, K. L. and Herschman, H. R. (1990) Nucleic Acids Res. **20**, 6049–6055

Anderson, M. E. (1985) Methods Enzymol. **113**, 548–555

Arseniev, A., Schultze, P., Worgotter, E., Braun, W., Wagner, G., Vasak, M., Kagi, J. H. R. and Wutrich, K. (1988) J. Mol. Biol. **201**, 637–657

Banci, L., Schröder, S. and Kollman, P. A. (1992) Proteins: Struct. Funct. Genet. **13**, 288–305

Brouwer, M. and Brouwer-Hoexum, T. (1991) Arch. Biochem. Biophys. **290**, 207–213

Brouwer, M. and Brouwer-Hoexum, T. (1992) Biochemistry **31**, 4096–4102

Brouwer, M., Schlenk, D., Ringwood, A. H. and Brouwer-Hoexum, T. M. (1992) Arch. Biochem. Biophys. **294**, 461–468

Brouwer, M., Brouwer-Hoexum, T. and Cashon, R. (1993) Mar. Environ. Res. **35**, 13–17

Butler, G. and Thiele, D. J. (1991) Mol. Cell. Biol. **11**, 476–485

Cismowski, M. J. and Huang, P. C. (1991) Biochemistry **30**, 6626–6632

Cismowski, M. J., Narula, S. S., Armitage, I. M., Chernaik, M. L. and Huang, P. C. (1991) J. Biol. Chem. **36**, 24390–24397

Coleman, J. (1992) Annu. Rev. Biochem. **61**, 897–946

Cousins, R. J. (1985) Physiol. Rev. **65**, 230–309

Creighton, T. E. (1986) Methods Enzymol. **131**, 83–106

Engel, D. W. and Brouwer, M. (1989) Adv. Comp. Environ. Physiol. **5**, 53–75

Fischer-Hjalmars, I. and Henriksson-Enflo, A. (1982) Adv. Quantum Chem. **16**, 1–42

Freedman, J. H., Ciriolo, M. R. and Peisach, J. (1989) J. Biol. Chem. **264**, 5598–5605

Gasteiger, J. and Marsili, M. (1980) Tetrahedron **36**, 3219–3228

Godwin, A. K., Meister, A., O'Dwyer, P. J., Huang, C. S., Hamilton, T. C. and Anderson, M. E. (1992) Proc. Natl. Acad. Sci. U.S.A. **89**, 3070–3074

Hagen, K. S., Stephan, D. W. and Holm, R. H. (1982) Inorg. Chem. **21**, 3928–3936

Hamer, D. H. (1986) Annu. Rev. Biochem. **55**, 913–951

Handbook of Chemistry and Physics (1984) (Weast, R. C., Astle, M. J. and Beyer, W. H., eds.), 65th edn., CRC Press, Boca Raton, Florida

Hoops, S. C., Anderson, K. W. and Merz, K. M., Jr. (1991) J. Am. Chem. Soc. **113**, 8262–8270

Kille, P., Lees, W. E., Darke, B. M., Winge, D. R., Dameron, C. T., Stephens, P. E. and Kay, J. (1992) J. Biol. Chem. **267**, 8042–8049

Kini, R. M. and Evans, H. J. (1991) J. Biomol. Struct. Dynamics **9**, 475–487

Kraker, A. J., Krakower, G., Shaw, C. F., III, Petering, D. H. and Garvey, J. (1988) Cancer Res. **48**, 3381–3388

Krezoski, S. K., Villalobos, J., Shaw, C. F. and Petering, D. H. (1988) Biochem. J. **255**, 483–491

Lange's Handbook of Chemistry (1973), (Dean, J. A., ed.) 11th edn., McGraw–Hill Book Company, New York

Lauher, J. W. (1986) J. Am. Chem. Soc. **108**, 1521–1531

Li, T. Y., Kraker, A. J., Shaw, C. F. and Petering, D. H. (1980) Proc. Natl. Acad. Sci. U.S.A. **77**, 6334–6338

Messerle, B. A., Schaffer, A., Vasak, M., Kagi, J. H. R. and Wuthrich, K. (1990) J. Mol. Biol. **214**, 765–779

Nielson, K. B., Atkin, C. L. and Winge, D. R. (1985) J. Biol. Chem. **260**, 5342–5350

Otvos, J. D. and Armitage, I. M. (1980) Proc. Natl. Acad. Sci. U.S.A. **77**, 7094–7098

Otvos, J. D., Olafson, R. W. and Armitage, I. M. (1982) J. Biol. Chem. **257**, 2427–2431

Otvos, J. D., Chen, S. and Liu, X. (1989) in Metal Ion Homeostasis, Molecular Biology and Chemistry (Winge, D. and Hamer, D., eds.), pp. 197–206, Alan R. Liss, New York

Robbins, A. H., McRee, D. E., Williamson, M., Collet, S. A., Xuong, N. H., Furey, W. F., Wang, B. C. and Stout, C. D. (1991) J. Mol. Biol. **221**, 1269–1293

Seguin, C. (1991) Gene **97**, 295–300

Shen, J., Wong, C. F., Subramaniam, S., Albright, T. A. and McCammon, J. A. (1990) J. Comp. Chem. **11**, 346–350

Singhal, R. K., Anderson, M. E. and Meister, A. (1987) FASEB J. **1**, 220–223

Steinkuhler, C., Sapora, O., Carri, M. T., Nagel, W., Marcocci, L., Ciriolo, M. R., Weser, U. and Rotilio, G. (1991) J. Biol. Chem. **266**, 24580–24587

Thiele, D. (1992) Nucleic Acids Res. **20**, 1183–1191

Vasak, M. (1986) Environ. Health Persp. **65**, 193–197

Vasak, M., Kägi, J. H. R. and Hill, H. A. O. (1981) Biochemistry **20**, 2852–2856

Waalkes, M. P. and Goering, P. L. (1990) Chem. Res. Toxicol. **3**, 281–288

Winge, D. R. and Miklossy, K.-A. (1982a) Arch. Biochem. Biophys. **214**, 80–88

Winge, D. R. and Miklossy, K.-A. (1982b) J. Biol. Chem. **257**, 3741–3746

Received 18 January 1993/8 March 1993; accepted 12 March 1993